

NUMERICAL AND EXPERIMENTAL MODELING OF SUBNANOSECOND PLASMA CLOSING SWITCHES IN GASES

J. H. Chen, C. J. Buchenauer, and J. S. Tyo

*Electrical and Computer Engineering Department, University of New Mexico,
Albuquerque, NM 87131*

Abstract

In this paper, a 2-D Finite Element Time Domain (FETD) model is presented for analyzing sub nanosecond plasma closing switches in gases, based on the Matlab Partial Differential Equation (PDE) toolbox. We will present the basic features of the model, as well as the results of validation studies on simple problems such as switch closure in an ideal, infinite, conically symmetric test volume. The physical model is then modified to simulate a test cell that had been previously used to collect experimental data. The dynamic channel current and its rate of the switch were evaluated based on the numerical model for different gases in different pressure regimes. The dynamics of the switch closure are greatly affected by the gas species and pressure used for insulation in the experiment.

I. INTRODUCTION

Measurement of the current-voltage (I-V) characteristics of sub-nanosecond plasma switches is very important. However, making these measurements directly can be challenging. Difficulties arise because of the structure of the switch, the high voltage, and the fast temporal signature with rise times that can be 100 ps or less. While the dynamics of closing switches in gases are well understood for switch closure times on the order of a few nanoseconds, there are relatively few studies examining the performance of such switches designed to close in times on the order of 100 ps. Such fast closing switches are important in a variety of pulsed power applications, including compact pulsed power and pulsers designed to drive ultra-wideband radiators. The dynamics of the channel after the initial closure event are also important for characterizing the losses inherent in the switch.

Recently, there was an extensive experimental study that made remote measurements of the induced electric field far from the channel that is created by a fast closing switch in low- and high-pressure nitrogen, hydrogen, helium and SF₆[1]. These measurements were made with a D-dot probe positioned approximately 60 mm from the switch closure location. Because of the structural design of the test chamber, the voltage and current characteristics of the channel cannot be determined directly from the measured fields. Instead, we are presented with the classic inverse problem of inferring the dynamics of the plasma channel from the remote measurements. In this paper, we present a numerical analysis of the test fixture constructed by Dick, *et al.*, [1], and use this information

to study the dynamic current characteristics of the channel in their experiments.

II. SIMULATION METHOD

Earlier research shows that a plasma channel is created when a switch closes, a radial electromagnetic wave is generated and propagates outwards from the plasma channel axis. The switch walls form a radial waveguide, which is a variable impedance structure causing continuous reflections as the wave propagates outward. Measurements of the output waveform normally include the superimposed effects of multiple reflections. Because of the above factors, a numerical model is a good tool that allows the measured electromagnetic fields to be related to the current in the plasma channel.

A. Modeling Method.

We choose Finite Element Method (FEM) in the time domain because it is well suited to the analysis of this particular problem. The finite element method can be performed on irregular meshes, making it useful for understanding the electromagnetic field effects near the feed point. The problem also has azimuthal symmetry; therefore, a 2-D (azimuthally symmetric) FETD model is chosen to describe the physical process.

Based on the Maxwell equations, the electric field \vec{E} and magnetic field \vec{H} can be solved from the following vector wave equations [2]

$$\nabla \times \left(\frac{1}{\mu} \nabla \times \vec{E} \right) + \epsilon \frac{d^2 \vec{E}}{dt^2} = - \frac{d\vec{J}}{dt} \quad (1)$$

$$\nabla \times \left(\frac{1}{\epsilon} \nabla \times \vec{H} \right) + \epsilon \frac{d^2 \vec{H}}{dt^2} = \nabla \times \left(\frac{1}{\epsilon} \vec{J} \right) \quad (2)$$

Where, \vec{J} is the plasma channel current density for simplicity, we assume a z-directed current channel, i.e. $\vec{J} = J_z \hat{z}$, so the magnetic field \vec{H} has only an azimuthal component. The electric field \vec{E} has two components \vec{E}_r and \vec{E}_z . We solve the vector wave equation in (1) using the FEM engine in the Matlab PDE Toolbox. Eq. (1) can be described by the standard hyperbolic PDE format (3) [3]

$$\mu\epsilon r \frac{\partial^2 u}{\partial t^2} - \nabla \cdot (r \nabla u) = -\mu \frac{\partial J}{\partial t}, \quad (3)$$

where r and z are the radial and axial coordinates in cylindrical coordinates and u represents each of the non zero components of the electric field. The boundary

conditions can be either Dirichlet (4) or Neumann (5), or a mixture of the two.

$$hu = r \quad (4)$$

$$\vec{n} \cdot (c\nabla u) + qu = g. \quad (5)$$

Equations (3) – (5) provide the standard vector hyperbolic PDE that is handled by the PDE Toolbox.

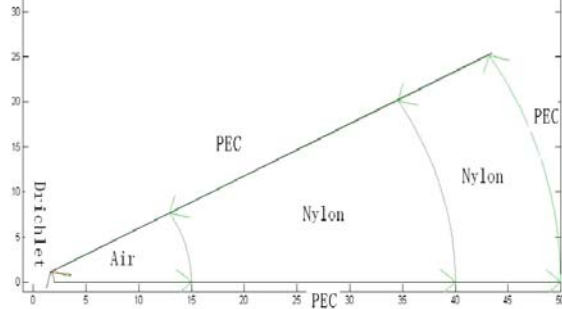
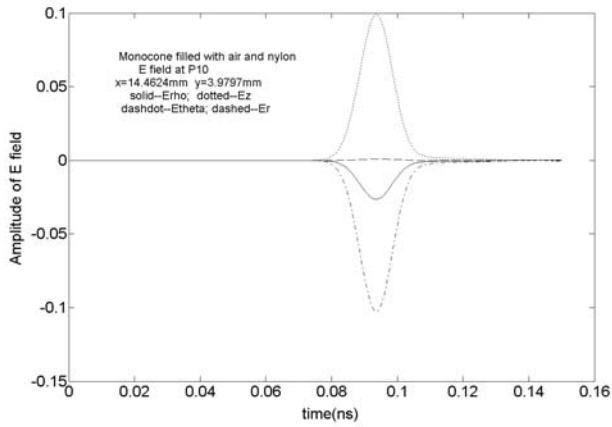
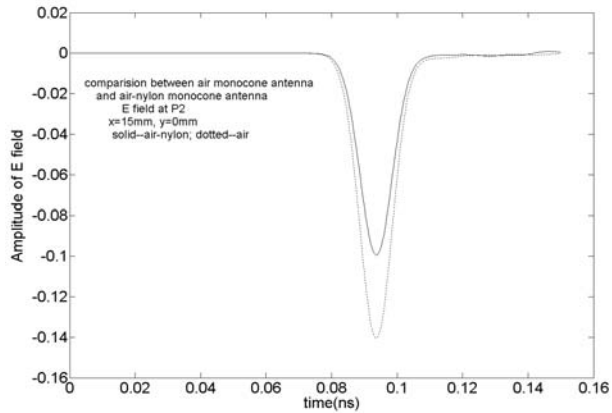


Figure 1 Geometry and boundary condition of a monocone antenna



(a)



(b)

Figure 2 (a) E field waveform inside monocone air-nylon antenna; (b)E field Comparison of air monocone and air-nylon monocone antenna

B. Model Verification

We verified the performance of our model by analyzing an ideal monocone excited by a Gaussian pulse. An ideal monocone excited at the feed carries only the TEM mode, and the voltage and current waveforms on the structure

are identical to the applied current. The geometry of our monocone is shown in figure 1. Note that nylon can be included to verify the performance of the model at the air-nylon interface. We analyzed the structure in figure 1 with and without the nylon. The simulation result is shown in figure 2 when the exciting wave is a Gaussian pulse. We can find that the propagating wave is almost completely TEM and the propagating waveform is a good replica of the applied Gaussian pulse. The simulation result is very close to the known analytical solution.

III. PHYSICAL MODEL AND SIMULATION RESULT

A. Test Switch.

The test switch used by Dick, *et al.*, [1] had a radial/conical transmission line topology. It contained a 20-mm-diameter gas cell and incorporated a dual transmission line structure from a profiled, cylindrical, nylon block, as shown in figure 3. The inner portion of this cylinder had parallel plates symmetry and formed a radial transmission line [4]. At a radial distance of 43 mm from the center of the cylinder, the profile changed to a conical transmission line filled with nylon ($\epsilon_r = 3.4$). The conical transmission line had an angle of 70° and so had a constant line impedance of 11.6Ω for the TEM mode. The upper and lower surfaces of the profiled nylon cylinder were covered with 0.08-mm-thick copper foil. The foil thickness is greater than the skin depth of copper for all frequencies greater than 673 kHz. The frequencies comprising the voltage collapse pulse are in the range of hundreds of MHz to a few GHz. The flat brass plates were 16 mm thick and 85 mm in diameter. There were two brass, hemispherical electrodes mounted (one on each plate) with a gap spacing of 0.7mm. D-dot monitors were situated 60 mm from the central switch axis to measure the voltage pulse using Tektronix SCD5000 and TDS220 oscilloscopes. The voltage induced in the monitor was

$$V_m = Z_0 I = Z_0 \frac{dQ}{dt} = Z_0 A_{eff} \frac{dD}{dt} = \epsilon A_{eff} Z_0 \frac{dE}{dt}. \quad (6)$$

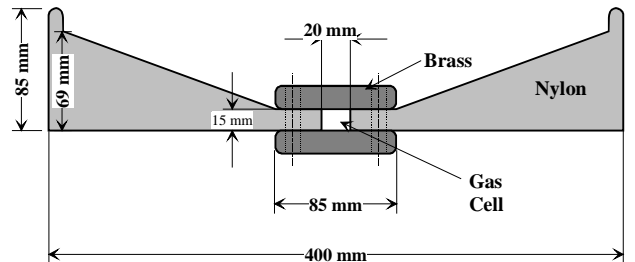


Figure 3. Geometry of test switch from [1].

B. Simulation and Deconvolution.

The first step in our analysis is to determine the response function that relates the measured field at the D-dot probe to the actual current flowing in the plasma channel. To accomplish this, we use a 63-ps-wide Gaussian pulse as

the exciting waveform. This pulse width is much narrower than the measured waveform, which helps with the stability of the deconvolution process.

The model of the test fixture was divided into three domains: 1) plasma channel region with a Gaussian pulse excitation, 2) gas region and 3) nylon region. We assumed PEC boundary conditions on upper and lower plates and cone surfaces. The outer wall was also described by PEC Boundary condition (it will be described by Absorbing Boundary Condition (ABC) in our future work). The lack of a good ABC forces us to only consider the early-time response of the system. However, we are mainly interested in the fast switch closure event, which is over long before the ~ 2 ns clear time of the model.

Figure 4 shows the E field inside the nylon cone at a distance of 60 mm from the channel. Note that while $E_r < E_\theta$, the radial component of the field is still significant. This means that the fields in the test fixture are not strictly TEM, and that a full-wave analysis is necessary to analyze the I-V characteristics. Furthermore, the pulse width increases from 63 ps at the feed to 78 ps at the sensor position.

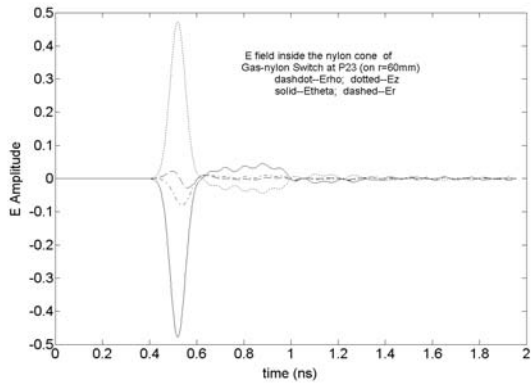


Figure 4. E Field Comparison on the interface between the Gas and Nylon inside the Switch

Figure 5 shows the process used to deduce the plasma channel current from the D-dot sensor response. A Gaussian plasma channel current (5(a)) radiates an E field (5(b)) at the D-dot sensor position. Based on linear

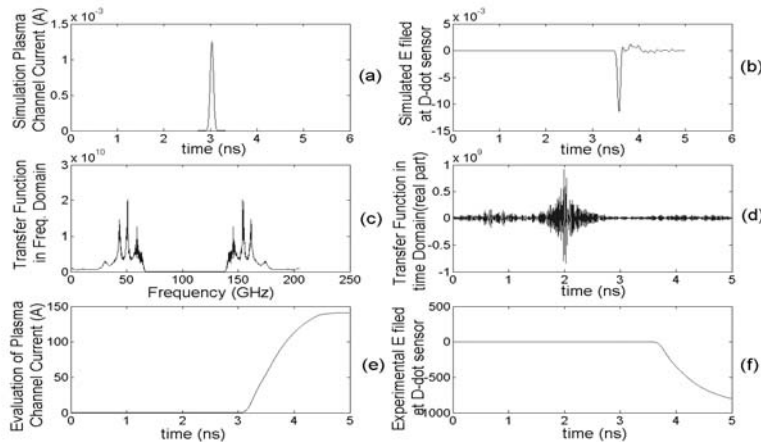


Figure 5. Deconvolution of Plasma Channel Current

systems theory, the inverse transfer function in frequency domain, (5(c)) can be deduced by dividing the measured E field by the applied current in the frequency domain. The inverse transfer function in the time domain is shown in Fig. 5(d). Even though the inverse transfer function has content up to ~ 60 GHz, the integrated measured waveforms had no energy at these frequencies, and hence, the SNR is large these higher frequencies. The physical plasma channel current (5(e)) can be deconvolved from the experimental E (5(f)). The experimental data in Fig. 5 comes from a high-pressure air-nylon switch filled with N_2 with the pressure of 49.3 bar at 65KV charge voltage. When we deduced the transfer function, the simulated E field was truncated before the wave reflected by the outer wall of the switch, which was set as Perfect Electric Conductor (PEC) boundary condition in the simulation, since we are most interested in the early time behavior in the switch.

IV. Discussion and Future Work

Figure 6 shows the evolution of the shape of dI/dt at different pressures for SF_6 . This process can be divided into 4 stages. Stage A –An initial fast transient pulse possibly due to leader formation dominates. (6(a)); Stage B – a later pulse indicative of actual switch closure begins to appear and is comparable to the initial pulse (6(b)); Stage C -- the 2nd pulse begins to dominate (6(c)); Stage D –the initial pulse is subsumed by the second pulse and is no longer visible (6(d)). The hydrogen, nitrogen and helium also have similar breakdown properties. The HWHM (half-width, half-maximum) pulse width is defined as shown in Figure 5. We use HWHM because the rising edge of the pulse is much faster than the falling edge, hence FWHM is not necessarily a good indicator of switch closure time. The experimental data in this figure and following figures are done with a 65 KV charge voltage and 0.7 mm gap spacing.

Figure 7 shows the HWHM time for different gases at different pressure. From this figure, we can how quickly each gas breaks down as a function of pressure. Hydrogen

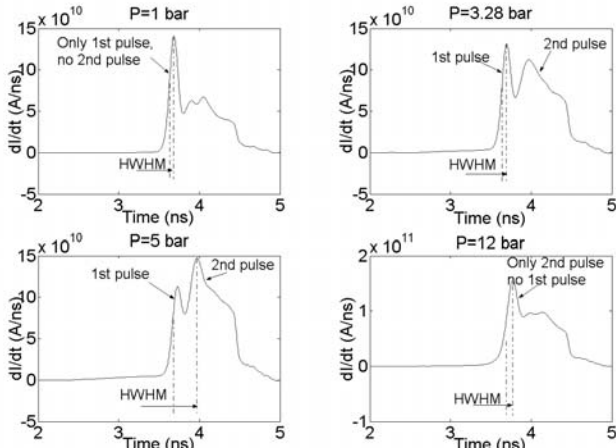


Fig. 6. Evolution of the dI/dt waveform for SF_6 with the Increasing Pressure

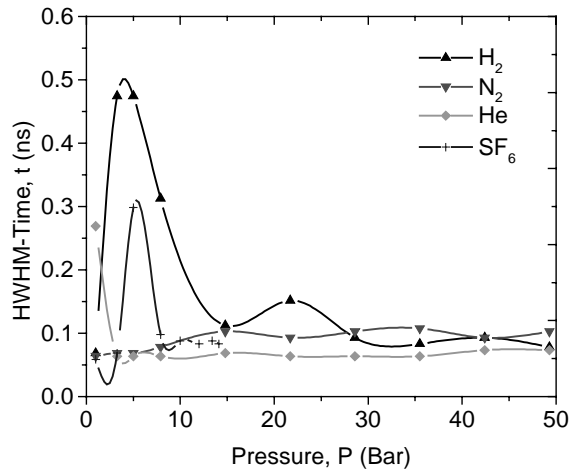


Figure 7. HWHM Time at Different Pressure/Gases

is fast to break down for the regime of stage A, then, it becomes slower as the pressure increases. When the pressure increases to about 6 bar, the stage C begins, and it is breaks down more quickly once again. Finally, when it enters into the regime of stage D, the dI/dt keeps almost the same shape; therefore, the HWHM time is almost constant as well. SF_6 has the same trend. The helium enters stage C when the pressure is 1 bar. Nitrogen's stage C almost happens after 21.7 bar, it is not as clear as with the other gases.

Figure 8 describes the maximum dI/dt for different gases at different pressure. For hydrogen, the dI/dt is mainly contributed by 1st, 1st, 2nd and 2nd pulse in stage A, B, C and D respectively. The variation with pressure is shown in table 1. ('+' means increase; '-' means decrease)

In this paper, the plasma channel current was assumed to be on the surface of a uniform cylinder. In the future, we hope to allow the conductivity and the channel size to

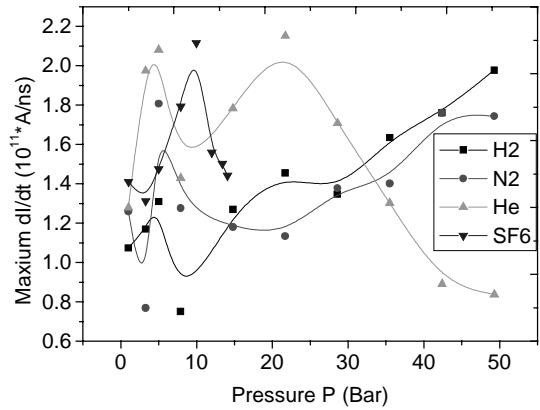


Fig. 8. Evaluated Maximum Plasma Channel Current at Different Pressure for Different Gases

Table 1 Maximum dI/dt for Different gases at Different Pressure

Stage	Hydrogen	Nitrogen	Helium	SF_6
A	+	+	N/A	N/A
B	+	-	N/A	-
C	-	N/A	+	+
D	+	+	-	-

vary dynamically so that we can compute the dynamic impedance of the channel, as well as the loss induced in the channel. Previous authors have proposed the Braginskii conduction model as a way to address this [5].

V. ACKNOWLEDGEMENTS

This work was supported by AFOSR under the MURI program and by Sandia National Lab under the Sandia University Researchers Program. The authors would like to express thanks to Drs. R. Pate and M. Kiefer of Sandia and Drs. S. J. MacGregor and A. R. Dick of Strathclyde University for access to their experimental measurements.

VI. REFERENCES

- [1]. Andrew R. Dick, Scott J. Macgregor et al, "Breakdown Phenomena in Ultra-Fast Plasma Closing Switches", IEEE Trans. Plasma Sci., Vol 28, NO. 5, Oct. 2000, pp. 1456-1462.
- [2]. Jianming Jin, "The Finite Element Method in Electromagnetics", 2nd Edition, John Wiley & Sons, Inc., 2002.
- [3]. "User's guide, Partial Differential Equation Toolbox", Version 1, Mathworks, 1996.
- [4]. S. J. Macgregor, A. R. Dick, "Final Report of High-Pressure Gas Switch Research for Sandia National Laboratories", ABQ, NM, Jan. 2001.
- [5] T. W. Hussey, *et al.*, "Dynamics of Nanosecond Spark Gap Channels," 1999 Pulsed Power Conference Digest, pp. 1171 – 1174 (1999)